Advances in Nano Research, *Vol. 7 No. 3 (2019) 145-155*
DOI: https://doi.org/10.12989/anr.2019.7.3.145

Dynamic modeling of smart magneto-electro-elastic curved nanobeams

Farzad Ebrahimi *1, Mohammad Reza Barati [1] and Vinyas Mahesh [2]

[1] *Mechanical Engineering Department, Faculty of Engineering, Imam Khomeini International University, Qazvin, P.O.B. 16818-34149, Iran*
[2] *Department of Mechanical Engineering, Nitte Meenakshi Institute of Technology, Karnataka 5600064, India*

(*Received October 6, 2018, Revised April 10, 2019, Accepted April 13, 2019*)

Abstract. In this article, the influence of small scale effects on the free vibration response of curved magneto-electro-elastic functionally graded (MEE-FG) nanobeams has been investigated considering nonlocal elasticity theory. Power-law is used to judge the through thickness material property distribution of MEE nanobeams. The Euler-Bernoulli beam model has been adopted and through Hamilton's principle the Nonlocal governing equations of curved MEE-FG nanobeam are obtained. The analytical solutions are obtained and validated with the results reported in the literature. Several parametric studies are performed to assess the influence of nonlocal parameter, magnetic potential, electric voltage, opening angle, material composition and slenderness ratio on the dynamic behaviour of MEE curved nanobeams. It is believed that the results presented in this article may serve as benchmark results in accurate analysis and design of smart nanostructures.

Keywords: curved nanobeam; free vibration; magneto-electro-elastic materials; functionally graded material; nonlocal elasticity

1. Introduction

In recent years, materials with designed mechanical and magneto-electrical properties have gained extensive attention. Magneto-electro-elastic functionally graded materials (MEE-FGMs) with continuous change in composition and properties in desired directions are employed to enhance the materials performance with sudden variations in material properties at the interfaces of multilayered piezoelectric structures (Vinyas and Kattimani 2017a, b, c, 2018a, b, Vinyas 2019a, b, Vinyas *et al*. 2018, 2019), On the other hand, the feature of continuous changes in material properties across the thickness coordinate leads to more complexities in analyzing such MEE-FG structures.

Nanobeams are one of the most important kinds of nanostructures which can be applied as building blocks for the fabrication of nanoelectromechanical systems (NEMs), Therefore, it is crucial to account for small scale effects in their mechanical analysis. The lack of a scale parameter in the classical continuum theory makes it impossible to describe the size effects. Hence, size dependent continuum theories such as nonlocal elasticity theory of Eringen (1972, 1983) and strain gradient theory (Li *et al*. 2015) are developed to consider the small scale effects. Lots of studies have been performed according to Eringen's nonlocal elasticity theory to investigate the size-dependent response of structural systems (Aydogdu 2009, Thai 2012), They indicated that nonlocal elastic models can only provide softening stiffness with increase of nonlocal parameter. For analysis of FGM nanostructures, nonlocal elasticity theory of Eringen is employed in many investigations. Şimşek and Yurtcu (2013) examined buckling behavior of FG nanobeams based on the nonlocal Timoshenko beam model. Rahmani and Jandaghian (2015) performed buckling analysis of FG nanobeams according to a nonlocal third-order shear deformable beam model. Li *et al*. (2016) analysed the free vibration response of FG Timoshenko beam under the framework of nonlocal strain gradient theory. Also, Li and Hu (2017) extended the evaluation to assess the torsional vibration of bi-directional FG nanotubes based on nonlocal elasticity theory. Semi-analytical vibration analysis of FG nanobeams is carried out by Ebrahimi *et al*. (2015), Thermal effects on vibration behavior of nonlocal temperature-dependent FGM nanobeams are investigated by Ebrahimi and Salari (2015a), Niknam and Aghdam (2015) studied nonlinear vibration response of nonlocal FG beams resting on elastic foundation. Ebrahimi and Barati (2017c) proposed a nonlocal third order beam model for vibration analysis of FG nanobeams. Also, investigation of buckling and vibration of smart piezoelectric and piezo-magnetic FG nanobeams attracted the attention of several researchers. Hosseini-Hashemi *et al*. (2014) explored surface effects on vibrational behavior of FG piezoelectric nanobeams using nonlocal elasticity. Ebrahimi and Salari (2015b) examined nonlocal thermo-electrical buckling behavior of FG piezoelectric nanobeams. Beni (2016) investigated buckling and vibration analysis of FG piezoelectric nanobeams. Also, Ebrahimi and Barati (2016) presented vibration analysis of a nanosize FG beam subjected to a magneto-electro-thermal loading. They indicated that vibration frequencies of straight FG nanobeams are affected by the sign and magnitude of electric voltage. More recently, it is shown that the nonlocal differential and integral elasticity based models may be not equivalent to each other (Zhu and Li

*Corresponding author, Ph.D., Professor,
E-mail: febrahimy@eng.ikiu.ac.ir

ISSN: 2287-237X (Print), 2287-2388 (Online)

2017a, b), Recently Ebrahimi and his co-workers performed some researches in the field of dispersion characteristics of waves propagating through composite nanosize beams and plates under various thermo-electro-magneto-elastic loadings via different nonlocal continuum theories (Ebrahimi *et al*. 2016a, b, 2018a, Ebrahimi and Dabbagh 2017a, b, c, d, 2018a, b, c, e, f, 2018b, Ebrahimi *et al*. 2016c, 2018b).

Due to the extensive application of FGM curved beams in different engineering areas, a deeper understanding of the mechanical behavior of such beams should be required. In recent years, curved nanobeams are applied in the nano-electro-mechanical systems (NEMS) due to possessing superior features than the straight nanobeams such as performance in large strokes and bi-stability nature. Such beams have practical applications in many systems such as nano-switches, nano-valves and nano-filters. A literature survey specifies that some research works address the vibration problem of isotropic curved nanobeams, rings, and arches. However, relatively few investigations are performed on vibration of FGM curved nanobeams. Assadi and Farshi (2011) explored vibration behavior of isotropic curved nanobeams and rings including surface energies. Yan and Jiang (2011) determined electromechanical response of curved piezoelectric nanobeams incorporating surface effects. Kananipour *et al*. (2014) applied the nonlocal elasticity to dynamic analysis of a curved nanobeam. Setoodeh *et al*. (2015) investigated thermal buckling of embedded curved nanotubes based on nonlocal Euler-Bernoulli beam model. Tufekci *et al*. (2016) presented static Analysis of nonlocal curved nanobeams with varying curvature and cross-section. Previously published works on mechanical analysis of nonlocal curved nanobeams indicate that increasing nonlocal parameter leads to stiffness softening effect. Therefore, they have not included any length scale parameter showing stiffness hardening effect reported in strain gradient theory. The above literature survey shows that the number of studies concerning with the behavior of straight FG nanobeams based on nonlocal elasticity theory is plenty; to the author's best knowledge, there are only few papers in the literature concerning with curved FG nanobeams. Hosseini and Rahmani (2016) makes the first attempt for free vibration analysis of deep curved FG nanobeams via a nonlocal curved beam model under simply-supported boundary conditions. They reported that vibration behavior of curved FG nanobeams is significantly affected by the value of opening angle and nonlocality parameter. So, there is no reported work relevant to the vibration of curved magneto-electro-elastic FG nanobeams incorporating nonlocal effects.

In this work, a size-dependent curved beam model is developed to take into account the effects of nonlocal stresses in vibration analysis of curved magneto-electro-elastic FG nanobeams for the first time. The governing differential equations are derived based on the principle of virtual work and Euler-Bernoulli beam theory. Power-law function is employed to describe the spatially graded magneto-electro-elastic properties. By extending the radius of curved nanobeam to infinity, the results of straight nonlocal FG beams can be rendered. The effects of magnetic potential, electric voltage, opening angle, nonlocal parameter, power-law index and slenderness ratio on vibration frequencies of curved MEE-FG nanobeams are studied.

2. Theory and formulation

2.1 The nonlocal elasticity model for magneto-electro-elastic nanobeams

Eringen's nonlocal theory (Eringen 1972, 1983) introduces the stress state at a point of body as a function of strains of all other points. For a nonlocal MEE structural element, the basic relations with zero body force can be expressed by

$$\begin{aligned}\sigma_{ij} = \int_V \alpha\left(|x'-x|,\tau\right)\big[&C_{ijkl}\varepsilon_{kl}(x') \\ &-e_{mij}E_m(x') - q_{nij}H_n(x')\big]dV(x')\end{aligned} \tag{1}$$

$$\begin{aligned}D_i = \int_V \alpha\left(|x'-x|,\tau\right)\big[&e_{ikl}\varepsilon_{kl}(x') \\ &+s_{im}E_m(x') + d_{in}H_n(x')\big]dV(x')\end{aligned} \tag{2}$$

$$\begin{aligned}B_i = \int_V \alpha\left(|x'-x|,\tau\right)\big[&q_{ikl}\varepsilon_{kl}(x') \\ &+d_{im}E_m(x') + \chi_{in}H_n(x')\big]dV(x')\end{aligned} \tag{3}$$

where σ_{ij}, ε_{ij}, D_i, E_i, B_i and H_i denote the stress, strain, electric displacement, electric field components, magnetic induction and magnetic field components, respectively; C_{ijkl}, e_{mij}, s_{im}, q_{nij}, d_{ij} and χ_{ij} are the elastic, piezoelectric, dielectric, piezomagnetic, magnetoelectric and magnetic constants, respectively; α ($|x' - x|$, τ) is the nonlocal kernel function and $|x' - x|$ is the Euclidean distance. Finally, the constitutive relations of a MEE solid can be expressed in an equivalent differential form as (Ebrahimi and Barati 2016)

$$\sigma_{ij} - (e_0\, a)^2\nabla^2\sigma_{ij} = C_{ijkl}\varepsilon_{kl} - e_{mij}E_m - q_{nij}H_n \tag{4}$$

$$D_i - (e_0\, a)^2\nabla^2 D_i = e_{ikl}\varepsilon_{kl} + s_{im}E_m + d_{in}H_n \tag{5}$$

$$B_i - (e_0\, a)^2\nabla^2 B_i = q_{ikl}\varepsilon_{kl} + d_{im}E_m + \chi_{in}H_n \tag{6}$$

where ∇^2 is the Laplacian operator and e_0a is nonlocal parameter which introduces the small size effect.

2.2 Effective properties of P-FGM curved nanobeam

Consider a curved FG nanobeam having length L and thickness h which its coordinates is depicted in Fig. 1. It is supposed that the material properties of curved MEE-FG nanobeam vary continuously through the thickness by a power law function. So, the material properties of nonlocal

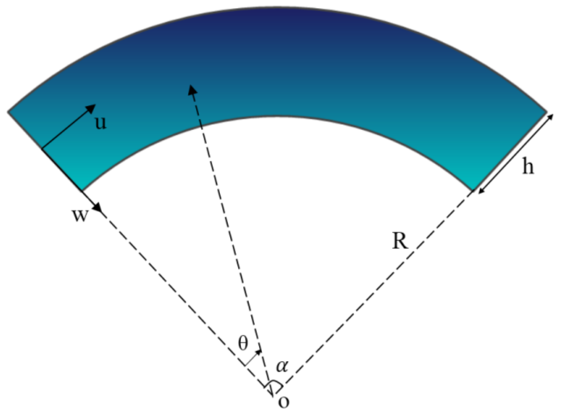

Fig. 1 Geometry and coordinates of curved FG nanobeam

Table 1 Magneto-electro -elastic coefficients of material properties

Properties	$BaTiO_3$	$CoFe_2O_4$
c_{11} (GPa)	166	286
e_{31} (Cm^{-2})	-4.4	0
q_{31} (N/Am)	0	580.3
s_{11} ($10^{-9}C^2m^{-2}N^{-1}$)	11.2	0.08
s_{33}	12.6	0.093
χ_{11} ($10^{-6}Ns^2C^{-2}/2$)	5	-590
χ_{33}	10	157
$d_{11} = d_{33}$	0	0
ρ (kgm^{-3})	5800	5300

MEE-FG beam P(z) such as elastic, piezomagnetic and magnetoelectric constants can be represented by (Ebrahimi and Barati 2017)

$$\mathrm{P}(z)=\left(\mathrm{P}_u-\mathrm{P}_l\right)\left(\frac{z}{h}+\frac{1}{2}\right)^p+\mathrm{P}_l \tag{7}$$

Here p is the power-law exponent which governs the graduation of material properties across the thickness. P_u and P_l denote the material property at top and bottom side, respectively. The top and bottom surfaces of curved FG nanobeam are supposed to be fully $BaTiO_3$ and fully $CoFe_2O_4$, respectively and their properties are listed in Table 1.

2.3 Kinematic relations

Based on curved Euler–Bernoulli beam model, the radial displacement w_r and tangential displacement u_θ can be written as

$$u_\theta\left(\theta,r,t\right)=(1+\frac{z}{R})u\left(\theta,t\right)+\frac{z}{R}(\frac{\partial w(\theta,t)}{\partial\theta}) \tag{8}$$

$$w_r(\theta,r,t)=-w(\theta,t) \tag{9}$$

where u and w denote displacement components of the mid-surface in tangential and radial directions, respectively. Satisfying Maxwell's equation in the quasi-static approximation gives the electric and magnetic field distributions across the thickness as follows (Ebrahimi and Barati 2016)

$$\Phi(x,z,t)=-\cos(\xi z)\phi(x,t)+\frac{2z}{h}V \tag{10}$$

$$\Upsilon(x,z,t)=-\cos(\xi z)\gamma(x,t)+\frac{2z}{h}\Omega \tag{11}$$

where $\xi = \pi / h$. Also, V and Ω are the external electric voltage and magnetic field intensity; ϕ and γ are the spatial function of the electric and magnetic potential, respectively.

The nonzero normal strain is

$$\varepsilon=\varepsilon^0+zk^0,$$
$$\varepsilon^0=\frac{1}{R}(-w+\frac{\partial u}{\partial\theta}),\qquad k^0=\frac{1}{R^2}(\frac{\partial u}{\partial\theta}+\frac{\partial^2 w}{\partial\theta^2}) \tag{12}$$

where ε^0 and k^0 denote the extensional and bending strains respectively.

According to the defined magneto-electric potential in Eqs. (10) and (11), the non-zero components of electric and magnetic fields (E_θ, E_z, H_θ, H_z) can be obtained as

$$\begin{aligned}E_\theta&=-\Phi_{,x}=\cos(\xi z)\frac{\partial\phi}{R\partial\theta},\\ E_z&=-\Phi_{,z}=-\xi\sin(\xi z)\phi-\frac{2V}{h}\end{aligned} \tag{13}$$

$$\begin{aligned}H_\theta&=-\Upsilon_{,x}=\cos(\xi z)\frac{\partial\gamma}{R\partial\theta},\\ H_z&=-\Upsilon_{,z}=-\xi\sin(\xi z)\gamma-\frac{2\Omega}{h}\end{aligned} \tag{14}$$

To derive the governing equation, Hamilton's principle is introduced as follows

$$\int_0^t\delta(\Pi_S-\Pi_K+\Pi_W)\,dt=0 \tag{15}$$

Here Π_S, Π_K and Π_W are strain energy, kinetic energy and external forces work, respectively. The strain energy can be written as

$$\begin{aligned}\delta\Pi_S=\int_v\sigma_{ij}\delta\varepsilon_{ij}\,dV=\int_v(\sigma_{\theta\theta}\delta\varepsilon_{\theta\theta}-D_\theta\delta E_\theta\\ -D_z\delta E_z-B_\theta\delta H_\theta-B_z\delta H_z)\,dV\end{aligned} \tag{16}$$

Inserting Eq. (14) into Eq. (11) gives

$$\begin{aligned}\delta\Pi_S=&\int_0^\alpha(N(\delta\varepsilon^0)+M(\delta k^0))Rd\theta\\ &+\int_0^\alpha\int_{-h/2}^{h/2}[-\frac{D_\theta}{R}\cos(\beta z)\delta\left(\frac{\partial\phi}{\partial\theta}\right)\end{aligned} \tag{17}$$

$$+D_z\beta\sin(\beta z)\delta\phi - \frac{B_\theta}{R}\cos(\beta z)\delta\left(\frac{\partial\gamma}{\partial\theta}\right) + B_z\beta\sin(\beta z)\delta\gamma]Rdzd\theta \quad (17)$$

in which N, Mrespectively denote the axial force and bending moment. The available stress resultants in Eq. (18) are defined by

$$N = \int_A \sigma_{xx}\, dA, \quad M = \int_A \sigma_{xx} z\, dA \quad (18)$$

The variation of kinetic energy is written as

$$\delta\Pi_K = \int_0^\alpha \left[I_0(\dot{u}\delta\dot{u} + \dot{w}\delta\dot{w}) + \frac{I_1}{R}(2\dot{u}\delta\dot{u} + \dot{u}\frac{\partial\delta\dot{w}}{\partial\theta} + \delta\dot{u}\frac{\partial\dot{w}}{\partial\theta}) + \frac{I_2}{R^2}(\dot{u}\delta\dot{u} + \dot{u}\frac{\partial\delta\dot{w}}{\partial\theta} + \delta\dot{u}\frac{\partial\dot{w}}{\partial\theta} + \frac{\partial\dot{w}}{\partial\theta}\frac{\partial\delta\dot{w}}{\partial\theta}\right] Rd\theta \quad (19)$$

where (I_0, I_1, I_2) are the mass moment of inertias, defined as follows

$$(I_0, I_1, I_2) = \int_A \rho(z)(1, z, z^2)\, dA \quad (20)$$

Thus, the variation works done by external loads can be written as

$$\delta\Pi_W = \int_0^L \frac{(N^E + N^M)}{R^2}(\frac{\partial w}{\partial\theta}\frac{\partial\delta w}{\partial\theta})Rd\theta \quad (21)$$

where N^E and N^M are applied electric and magnetic loads which is defined as

$$N^E = -\int_{-h/2}^{h/2} e_{31}\frac{2V}{h}dz \quad (22)$$

$$N^M = -\int_{-h/2}^{h/2} q_{31}\frac{2\Omega}{h}dz \quad (23)$$

The nonlocal constitutive relations (8) and (9) may be rewritten for a curved Magneto-electro-elastic Euler-Bernoulli nanobeam as

$$\sigma_{\theta\theta} - \mu\frac{\partial^2\sigma_{\theta\theta}}{R^2\partial\theta^2} = c_{11}\varepsilon_{\theta\theta} - e_{31}E_z - q_{31}H_z \quad (24)$$

$$D_\theta - \mu\frac{\partial^2 D_\theta}{R^2\partial\theta^2} = s_{11}E_\theta + d_{11}H_\theta \quad (25)$$

$$D_z - \mu\frac{\partial^2 D_z}{R^2\partial\theta^2} = e_{31}\varepsilon_{\theta\theta} + s_{33}E_z + d_{33}H_z \quad (26)$$

$$B_\theta - \mu\frac{\partial^2 B_\theta}{R^2\partial\theta^2} = d_{11}E_\theta + \chi_{11}H_\theta \quad (27)$$

$$B_z - \mu\frac{\partial^2 B_z}{R^2\partial\theta^2} = q_{31}\varepsilon_{\theta\theta} + d_{33}E_z + \chi_{33}H_z \quad (28)$$

where μ = ea^2. The following governing equations are obtained by inserting Eqs. (17)-(21) in Eq. (15) when the coefficients of δu, δw and $\delta\phi$ are equal to zero

$$-\frac{\partial N}{\partial\theta} - \frac{1}{R}\frac{\partial M}{\partial\theta} = -RI_0\ddot{u} - I_1(2\ddot{u} + \frac{\partial\ddot{w}}{\partial\theta}) - \frac{I_2}{R}(\ddot{u} + \frac{\partial\ddot{w}}{\partial\theta}) \quad (29)$$

$$\frac{1}{R}\frac{\partial^2 M}{\partial\theta^2} - N - \frac{(N^E + N^M)}{R}\frac{\partial^2 w}{\partial\theta^2} = -RI_0\ddot{w} + I_1\frac{\partial\ddot{u}}{\partial\theta} + \frac{I_2}{R}(\frac{\partial^2\ddot{w}}{\partial\theta^2} + \frac{\partial\ddot{u}}{\partial\theta}) \quad (30)$$

$$\int_{-h/2}^{h/2}\left(\cos(\beta z)\frac{1}{R}\frac{\partial D_\theta}{\partial\theta} + \beta\sin(\beta z)D_z\right)dz = 0 \quad (31)$$

$$\int_{-h/2}^{h/2}\left(\cos(\beta z)\frac{1}{R}\frac{\partial B_\theta}{\partial\theta} + \beta\sin(\beta z)B_z\right)dz = 0 \quad (32)$$

Under the following boundary conditions

$$N + \frac{M}{R} = 0 \quad \text{or} \quad u = 0 \quad \text{at} \quad \theta = 0 \quad \text{and} \quad \theta = \alpha \quad (33)$$

$$\frac{\partial M}{R\partial x} + I_1\ddot{u} + \frac{I_2}{R}(\ddot{u} + \frac{\partial\ddot{w}}{\partial x}) = 0 \quad \text{or} \quad w = 0 \quad \text{at} \quad \theta = 0 \quad \text{and} \quad \theta = \alpha \quad (34)$$

$$M = 0 \quad \text{or} \quad \frac{\partial w}{\partial\theta} = 0 \quad \text{at} \quad \theta = 0 \quad \text{and} \quad \theta = \alpha \quad (35)$$

$$\int_A D_\theta\cos(\beta z)\, dA = 0 \quad \text{or} \quad \phi = 0 \quad \text{at} \quad \theta = 0 \quad \text{and} \quad \theta = \alpha \quad (36)$$

$$\int_A B_\theta\cos(\beta z)\, dA = 0 \quad \text{or} \quad \gamma = 0 \quad \text{at} \quad \theta = 0 \quad \text{and} \quad \theta = \alpha \quad (37)$$

By integrating Eqs. (24)-(28) over the area of nanobeam's cross-section, the following relations for the nonlocal FG beam can be obtained

$$N - \mu\frac{\partial^2 N}{R^2\partial\theta^2} = \frac{A_{11}}{R}(-w + \frac{\partial u}{\partial\theta}) + \frac{B_{11}}{R^2}(\frac{\partial u}{\partial\theta} + \frac{\partial^2 w}{\partial\theta^2}) + A_{31}^e\phi + A_{31}^m\gamma - N_x^E - N_x^M \quad (38)$$

$$M - \mu\frac{\partial^2 M}{R^2\partial\theta^2} = \frac{B_{11}}{R}(-w + \frac{\partial u}{\partial\theta}) + \frac{D_{11}}{R^2}(\frac{\partial u}{\partial\theta} + \frac{\partial^2 w}{\partial\theta^2}) + E_{31}^e\phi + E_{31}^m\gamma - M_x^E - M_x^M \quad (39)$$

$$\int_{-h/2}^{h/2}\left\{D_\theta - \frac{\mu}{R^2}\frac{\partial^2 D_\theta}{\partial\theta^2}\right\}\cos(\xi z)dz = +\frac{F_{11}^e}{R}\frac{\partial\phi}{\partial\theta} + \frac{F_{11}^m}{R}\frac{\partial\gamma}{\partial\theta} \quad (40)$$

$$\begin{aligned}&\int_{-h/2}^{h/2}\left\{D_z-\frac{\mu}{R^2}\frac{\partial^2 D_z}{\partial\theta^2}\right\}\xi\sin(\xi z)dz\\&=\frac{A_{31}^e}{R}(-w+\frac{\partial u}{\partial\theta})+\frac{E_{31}^e}{R^2}(\frac{\partial u}{\partial\theta}+\frac{\partial^2 w}{\partial\theta^2})-F_{33}^e\phi-F_{33}^m\gamma\end{aligned}\tag{41}$$

$$\int_{-h/2}^{h/2}\left\{B_\theta-\frac{\mu}{R^2}\frac{\partial^2 B_\theta}{\partial\theta^2}\right\}\cos(\xi z)dz=+\frac{F_{11}^m}{R}\frac{\partial\phi}{\partial\theta}+\frac{X_{11}^m}{R}\frac{\partial\gamma}{\partial\theta}\tag{42}$$

$$\begin{aligned}&\int_{-h/2}^{h/2}\left\{B_z-\frac{\mu}{R^2}\frac{\partial^2 B_z}{\partial\theta^2}\right\}\xi\sin(\xi z)dz\\&=\frac{A_{31}^m}{R}(-w+\frac{\partial u}{\partial\theta})+\frac{E_{31}^m}{R^2}(\frac{\partial u}{\partial\theta}+\frac{\partial^2 w}{\partial\theta^2})-F_{33}^m\phi-X_{33}^m\gamma\end{aligned}\tag{43}$$

The cross-sectional rigidities are defined as follows

$$(A_{11},B_{11},D_{11})=\int_{-h/2}^{h/2}c_{11}(z)(1,z,z^2)dz\tag{44}$$

$$\left\{A_{31}^e,E_{31}^e\right\}=\int_{-h/2}^{h/2}e_{31}\left\{\xi\sin(\xi z),z\xi\sin(\xi z)\right\}dz\tag{45}$$

$$\left\{A_{31}^m,E_{31}^m\right\}=\int_{-h/2}^{h/2}q_{31}\left\{\xi\sin(\xi z),z\xi\sin(\xi z)\right\}dz\tag{46}$$

$$\left\{F_{11}^e,F_{33}^e\right\}=\int_{-h/2}^{h/2}\left\{s_{11}\cos^2(\xi z),s_{33}\xi^2\sin^2(\xi z)\right\}dz\tag{47}$$

$$\left\{F_{11}^m,F_{33}^m\right\}=\int_{-h/2}^{h/2}\left\{d_{11}\cos^2(\xi z),d_{33}\xi^2\sin^2(\xi z)\right\}dz\tag{48}$$

$$\left\{X_{11}^m,X_{33}^m\right\}=\int_{-h/2}^{h/2}\left\{\chi_{11}\cos^2(\xi z),\chi_{33}\xi^2\sin^2(\xi z)\right\}dz\tag{49}$$

And

$$N_x^E=-\int_{-h/2}^{h/2}e_{31}\frac{2V}{h}dz,\ N_x^M=-\int_{-h/2}^{h/2}q_{31}\frac{2\Omega}{h}dz\tag{50}$$

$$M_x^E=-\int_{-h/2}^{h/2}e_{31}\frac{2V}{h}zdz,\ M_x^M=-\int_{-h/2}^{h/2}q_{31}\frac{2\Omega}{h}zdz\tag{51}$$

The governing equations of a curved MEE-FG nanobeam can be obtained inserting Eqs. (38)-(43), respectively, into Eqs. (29)-(32) as

$$\begin{aligned}&\frac{A_{11}}{R}(-\frac{\partial w}{\partial\theta}+\frac{\partial^2 u}{\partial\theta^2})+\frac{B_{11}}{R^2}(-\frac{\partial w}{\partial\theta}+2\frac{\partial^2 u}{\partial\theta^2}+\frac{\partial^3 w}{\partial\theta^3})\\&+\frac{D_{11}}{R^3}(\frac{\partial^2 u}{\partial\theta^2}+\frac{\partial^3 w}{\partial\theta^3})+A_{31}^e\frac{\partial\phi}{\partial\theta}+\frac{E_{31}^e}{R}\frac{\partial\phi}{\partial\theta}+A_{31}^m\frac{\partial\gamma}{\partial\theta}+\frac{E_{31}^m}{R}\frac{\partial\gamma}{\partial\theta}\\&-RI_0\ddot{u}-I_1(2\ddot{u}+\frac{\partial\ddot{w}}{\partial\theta})-\frac{I_2}{R}(\ddot{u}+\frac{\partial\ddot{w}}{\partial\theta})+\frac{\mu}{R^2}(+RI_0\frac{\partial^2\ddot{u}}{\partial\theta^2}+\\&I_1(2\frac{\partial^2\ddot{u}}{\partial\theta^2}+\frac{\partial^3\ddot{w}}{\partial\theta^3})+\frac{I_2}{R}(\frac{\partial^2\ddot{u}}{\partial\theta^2}+\frac{\partial^3\ddot{w}}{\partial\theta^3})=0\end{aligned}\tag{52}$$

$$\begin{aligned}&\frac{A_{11}}{R}(-w+\frac{\partial u}{\partial\theta})+\frac{B_{11}}{R^2}(\frac{\partial u}{\partial\theta}+2\frac{\partial^2 w}{\partial\theta^2}-\frac{\partial^3 u}{\partial\theta^3})\\&-\frac{D_{11}}{R^3}(\frac{\partial^3 u}{\partial\theta^3}+\frac{\partial^4 w}{\partial\theta^4})-\frac{E_{31}^e}{R}\frac{\partial^2\phi}{\partial\theta^2}+A_{31}^e\phi\\&-\frac{E_{31}^m}{R}\frac{\partial^2\gamma}{\partial\theta^2}+A_{31}^m\gamma-RI_0\ddot{w}+I_1\frac{\partial\ddot{u}}{\partial\theta}\\&+\frac{I_2}{R}(\frac{\partial^2\ddot{w}}{\partial\theta^2}+\frac{\partial\ddot{u}}{\partial\theta})+(\frac{N^E}{R})\frac{\partial^2 w}{\partial\theta^2}+\frac{\mu}{R^2}(+RI_0\ddot{w}-I_1\frac{\partial\ddot{u}}{\partial\theta}\\&-I_1\frac{\partial\ddot{u}}{\partial\theta}-\frac{I_2}{R}(\frac{\partial^2\ddot{w}}{\partial\theta^2}+\frac{\partial\ddot{u}}{\partial\theta})-(\frac{N^E}{R})\frac{\partial^4 w}{\partial\theta^4})=0\end{aligned}\tag{53}$$

$$\begin{aligned}&\frac{F_{11}^e}{R}\frac{\partial^2\phi}{\partial\theta^2}+\frac{F_{11}^m}{R}\frac{\partial^2\gamma}{\partial\theta^2}+A_{31}^e(-w+\frac{\partial u}{\partial\theta})\\&+\frac{E_{31}^e}{R}(\frac{\partial u}{\partial\theta}+\frac{\partial^2 w}{\partial\theta^2})-RF_{33}^e\phi-RF_{33}^m\gamma=0\end{aligned}\tag{54}$$

$$\begin{aligned}&\frac{F_{11}^m}{R}\frac{\partial^2\phi}{\partial\theta^2}+\frac{X_{11}^m}{R}\frac{\partial^2\gamma}{\partial\theta^2}+A_{31}^m(-w+\frac{\partial u}{\partial\theta})\\&+\frac{E_{31}^m}{R}(\frac{\partial u}{\partial\theta}+\frac{\partial^2 w}{\partial\theta^2})-RF_{33}^m\phi-RX_{33}^m\gamma=0\end{aligned}\tag{55}$$

3. Solution procedure

In this section, analytical solution has been employed to solve the nonlocal governing equations of curved MEE-FG nanobeam with simply-simply supported boundary edges. To satisfy the boundary conditions, the following solution for displacement variables is employed

$$u(\theta,t)=\sum_{n=1}^{\infty}U_n\,\mathrm{Cos}[\frac{n\pi}{\theta}\alpha]e^{i\omega_n t}\tag{56}$$

$$w(\theta,t)=\sum_{n=1}^{\infty}W_n\,\mathrm{Sin}[\frac{n\pi}{\theta}\alpha]e^{i\omega_n t}\tag{57}$$

$$\phi(\theta,t)=\sum_{n=1}^{\infty}\Phi_n\,\mathrm{Sin}[\frac{n\pi}{\theta}\alpha]e^{i\omega_n t}\tag{58}$$

$$\gamma(\theta,t)=\sum_{n=1}^{\infty}\Upsilon_n\,\mathrm{Sin}[\frac{n\pi}{\theta}\alpha]e^{i\omega_n t}\tag{59}$$

in which (U_n, W_n, Φ_n, Υ_n) are the unknown Fourier coefficients. Inserting Eqs. (56) and (59) into Eqs. (52) to (55) respectively, leads to

$$\left\{[K]+[M]\omega^2\right\}\begin{Bmatrix}U_n\\W_n\end{Bmatrix}=0\tag{60}$$

where [K] and [M] are the stiffness and mass matrixes for FG nanobeam, respectively.

$$k_{1,1}=-\frac{A_{11}}{R}\left(\frac{n\pi}{\theta}\alpha\right)^2-\frac{2B_{11}}{R^2}\left(\frac{n\pi}{\theta}\alpha\right)^2+\frac{D_{11}}{R^3}\left(\frac{n\pi}{\theta}\alpha\right)$$

$$\begin{aligned}k_{1,2}=&-\frac{A_{11}}{R}\left(\frac{n\pi}{\theta}\alpha\right)-\frac{B_{11}}{R^2}\left(\frac{n\pi}{\theta}\alpha\right)\\&-\frac{B_{11}}{R^2}\left(\frac{n\pi}{\theta}\alpha\right)^3-\frac{D_{11}}{R^3}\end{aligned}$$

Table 2 Comparison of dimensionless frequency of curved FG nanobeam for various opening angles and nonlocal parameters (L/h = 50)

μ	$\alpha = \pi/3$, p = 0		$\alpha = \pi/4$, p = 0.5		$\alpha = \pi/2$, p = 1		$\alpha = 2\pi/3$, p = 5	
	Hosseini and Rahmani 2016	Present	Hosseini and Rahmani 2016	Present	Hosseini and Rahmani 2016	Present	Hosseini and Rahmani 2016	Present
0	8.31770	8.32132	7.30721	7.31014	4.72079	4.72275	2.63872	2.64019
1	7.93532	7.93877	6.97129	6.97408	4.50376	4.50563	2.51741	2.51881
2	7.60125	7.60455	6.67780	6.68048	4.31416	4.31595	2.41143	2.41277
3	7.30611	7.30928	6.41852	6.42108	4.14665	4.14837	2.3178	2.31909

$$k_{1,3} = -A_{31}^{e}\left(\frac{n\pi}{\theta}\alpha\right) - \frac{E_{31}^{e}}{R}\left(\frac{n\pi}{\theta}\alpha\right),$$

$$k_{1,4} = -A_{31}^{m}\left(\frac{n\pi}{\theta}\alpha\right) - \frac{E_{31}^{m}}{R}\left(\frac{n\pi}{\theta}\alpha\right)$$

$$k_{2,2} = -\frac{A_{11}}{R} - \frac{2B_{11}}{R^2}\left(\frac{n\pi}{\theta}\alpha\right)^2 - \frac{D_{11}}{R^3}\left(\frac{n\pi}{\theta}\alpha\right)^4$$
$$-\frac{N^E + N^M}{R}(1 + \frac{\mu}{R^2}\left(\frac{n\pi}{\theta}\alpha\right)^2)\left(\frac{n\pi}{\theta}\alpha\right)^2$$

$$k_{2,3} = -A_{31}^{e} - \frac{E_{31}^{e}}{R}\left(\frac{n\pi}{\theta}\alpha\right)^2,$$

$$k_{2,4} = -A_{31}^{m} - \frac{E_{31}^{m}}{R}\left(\frac{n\pi}{\theta}\alpha\right)^2$$

$$k_{3,3} = -\frac{F_{11}^{e}}{R}\left(\frac{n\pi}{\theta}\alpha\right)^2 - RF_{33}^{e},$$

$$k_{3,4} = -\frac{F_{11}^{m}}{R}\left(\frac{n\pi}{\theta}\alpha\right)^2 - RF_{33}^{m},$$

$$k_{4,4} = -\frac{X_{11}^{m}}{R}\left(\frac{n\pi}{\theta}\alpha\right)^2 - RX_{33}^{m}$$

$$m_{1,1} = +(RI_0 + I_1 + \frac{I_2}{R})\omega^2(1 + \frac{\mu}{R^2}\left(\frac{n\pi}{\theta}\alpha\right)^2)$$

$$m_{1,2} = +\left(I_1 + \frac{I_2}{R}\right)\omega^2(1 + \frac{\mu}{R^2}\left(\frac{n\pi}{\theta}\alpha\right)^2)\left(\frac{n\pi}{\theta}\alpha\right)$$

$$m_{2,2} = +RI_0\omega^2(1 + \frac{\mu}{R^2}\left(\frac{n\pi}{\theta}\alpha\right)^2)$$
$$+\frac{I_2}{R}\omega^2(1 + \frac{\mu}{R^2}\left(\frac{n\pi}{\theta}\alpha\right)^2)\left(\frac{n\pi}{\theta}\alpha\right)^2$$

$$m_{2,3} = m_{1,3} = m_{3,2} = m_{3,1} = m_{3,3} = m_{3,4} = m_{4,3} = m_{4,4} = 0$$

Also, for nontrivial solution of Eq. (49), the determinant $|[K] + [M]\omega^2|$ should be zero to obtain natural frequencies.

4. Numerical results and discussions

In this section, we examine vibrational behavior of a nonlocal curved MEE-FG nanobeam subjected to the magneto-electrical field. The length of curved nanobeam is L = 10 nm. For the validation purpose, the frequency results of present paper are validated with those of curved FG nanobeams presented by Hosseini and Rahmani (2016) using nonlocal elasticity theory of Eringen. They used the material properties as: E_m = 70 GPa, ρ_m = 2702 kgm^{-3} for metallic phase and E_c = 427 GPa, ρ_c = 3960 kgm^{-3} for ceramic phase. Table 2 presents the comparison results for a curved FG nanobeam with S-S boundary conditions and various nonlocal parameters and a good agreement is observed. So, the present paper can accurately predict mechanical behavior of curved FG nanobeams. Calculations are performed adopting the non-dimensional form of natural frequencies

$$\tilde{\omega} = \omega L^2\sqrt{\frac{\rho^u A}{c_{11}^u I}} \tag{61}$$

Figs. 2 and 3 show the variation of dimensionless frequency of curved MEE-FG nanobeam respectively versus applied voltage (V) and magnetic potential (Ω) for various values of opening angle ($\alpha = \pi/4$, $\pi/3$, $\pi/2$, $2\pi/3$) at μ = 1 nm^2, p = 1 and L/h = 20. It is observable that increasing applied voltage leads to smaller dimensionless frequencies.

But, magnetic field has an opposite effect on vibration frequencies. So, increasing magnetic potential leads to enlargement of dimensionless frequency for every value of opening angle. Also, as the value of opening angle increases, the magnitude of dimensionless frequency reduces. So, curvature of MEE-FG nanobeams plays a major

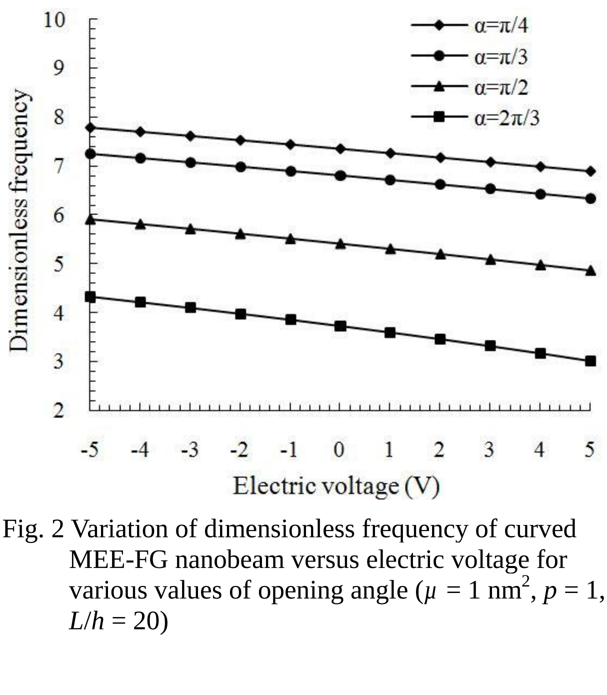

Fig. 2 Variation of dimensionless frequency of curved MEE-FG nanobeam versus electric voltage for various values of opening angle (μ = 1 nm^2, p = 1, L/h = 20)

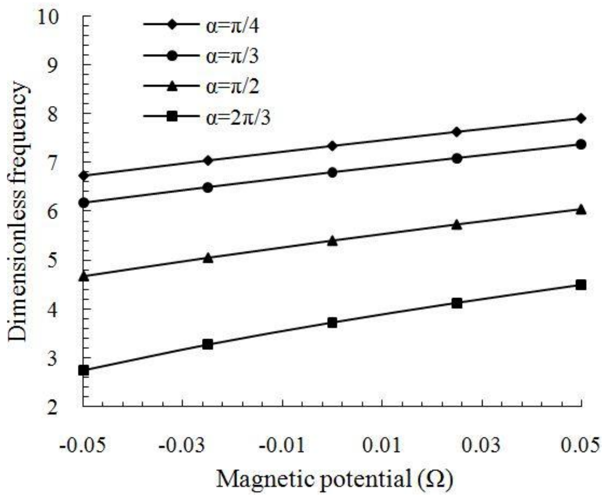

Fig. 3 Variation of dimensionless frequency of curved MEE-FG nanobeam versus magnetic potential for various values of opening angle (μ = 1 nm^2, p = 1, L/h = 20, V = 0)

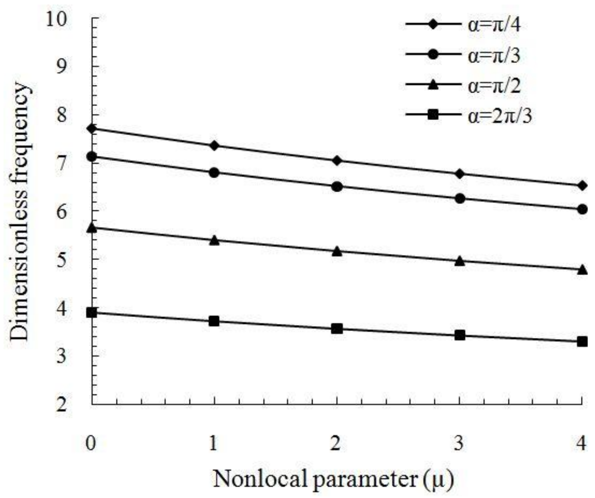

Fig. 4 Variation of dimensionless frequency of curved MEE-FG nanobeam versus nonlocal parameter for various values of opening angle (p = 1, L/h = 20, V = Ω = 0)

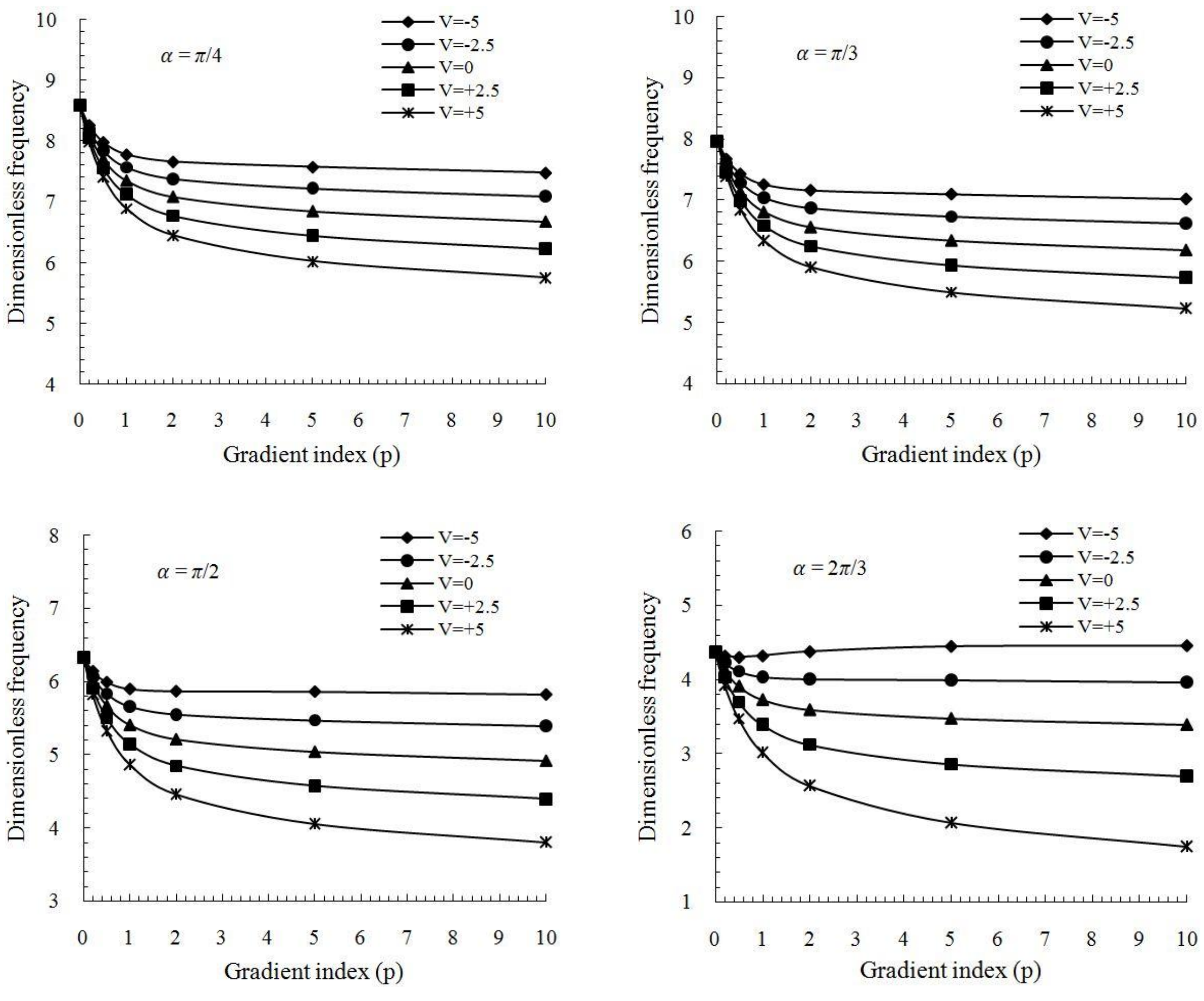

Fig. 5 Variation of dimensionless frequency of curved MEE-FG nanobeam versus gradient index for various values of opening angle and electric voltage (μ = 1 nm^2, L/h = 20)

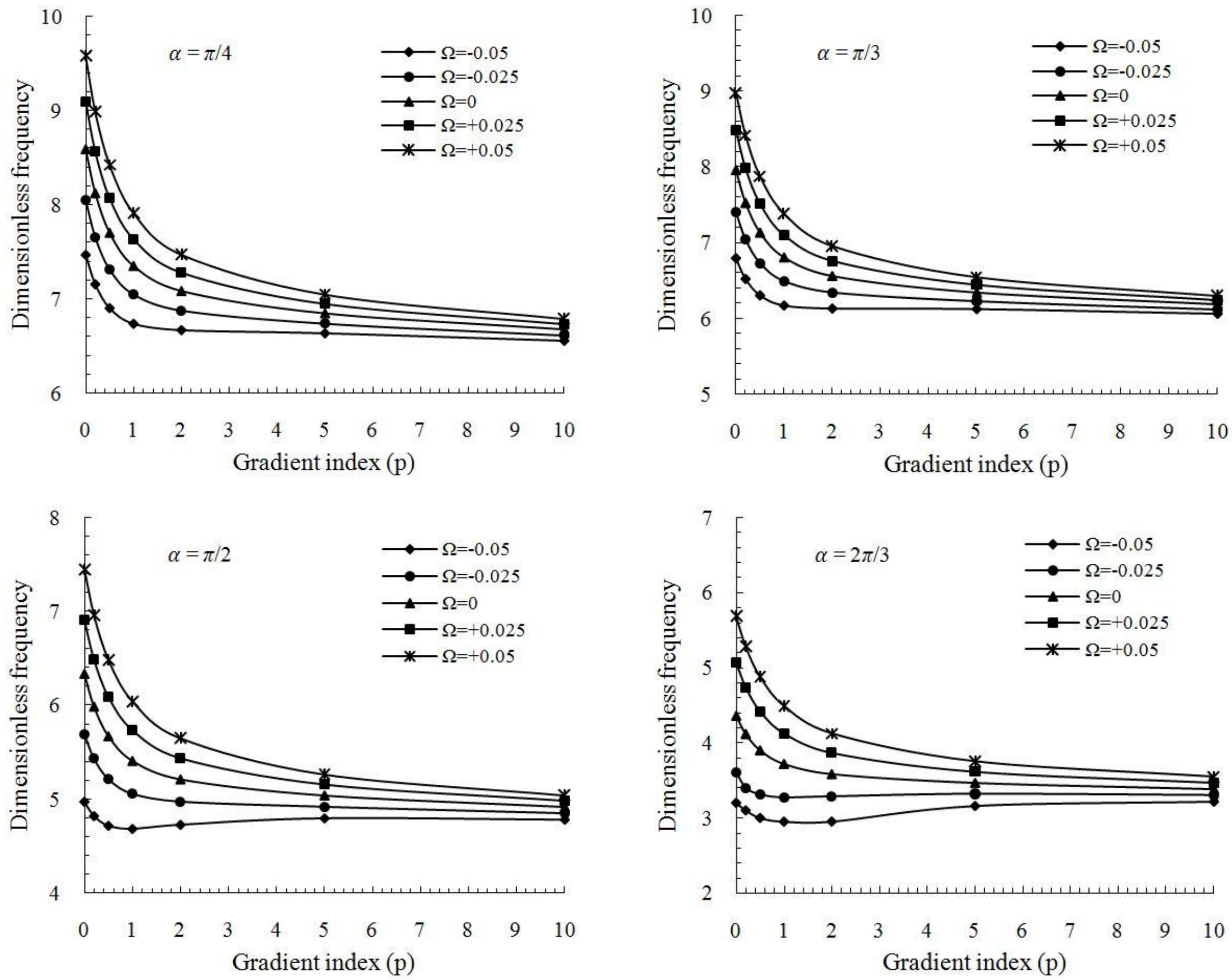

Fig. 6 Variation of dimensionless frequency of curved MEE-FG nanobeam versus gradient index for various values of opening angle and magnetic potential(μ = 1 nm^2, L/h = 20)

role in their vibration behavior. In fact, the difference in frequency results is more significant according to higher opening angles at a fixed electric voltage and magnetic potential. For example, the difference in natural frequency between $\alpha = \pi/4$ and $\pi/3$ is less than those observed between $\alpha = \pi/2$ and $2\pi/3$. Generally, effect of opening angle on vibration behavior becomes more significant as its value increase.

Fig. 4 depicts the variation of dimensionless frequency of S-S curved MEE-FG nanobeam versus nonlocal parameter (μ) for different values of opening angle (α) at gradient index p = 1 and slenderness ratio L/h = 20. As previously specified, for all values of nonlocality parameters, increasing opening angle (α) leads to lower dimensionless frequencies. A rise in nonlocal parameter leads to smaller values of dimensionless frequency. The reason is lower stiffness of curved nanobeam when it becomes smaller. This phenomenon shows that the curved MEE-FG nanobeam exerts a stiffness-softening effect when nonlocal parameter increases. Effect of material gradient index (p) on dimensionless frequency of curved MEE-FG nanobeam for various values of electric voltage and opening angle ($\alpha = \pi/4, \pi/3, \pi/2, 2\pi/3$) at L/h = 20 and μ = 1 nm^2 is plotted in Fig. 5. It is observable that for all values of electric voltage the frequency degrades with the gradient index enlargement, significantly for smaller gradient indices. The reason is higher portion of $CoFe_2O_4$ phase as the value of gradient index increases. Also, it is clear that effect of material composition index (p) on vibration frequencies depends on the sign and value of electric voltage. Reduction in dimensionless frequency with respect to gradient index (p) is more significant according to positive voltages which shows the notability of the sign of external electric voltage.

Fig. 6 illustrates the variation of dimensionless frequency of curved MEE-FG nanobeam versus gradient index (p) for various values of opening angle and magnetic potential at μ = 1 nm^2 and L/h = 20. It is observable that for every value of magnetic potential, dimensionless frequency degrades vigorously for smaller gradient indices and then reduces monotonically for larger gradient indices. Also, it is found that the reduction in natural frequency is more announced according to the negative magnetic potentials for every value of opening angle. So, the vibration frequencies become closer together at larger gradient indices.

Another investigation concerning with the effect of material composition and magneto-electrical field on vibration frequencies of curved MEE-FG nanobeam is presented in Figs. 7 and 8 when μ = 1 nm^2, $\alpha = \pi/4$ and L/h = 20. When p = 0, applied voltage has no influence on vibration frequencies due to the reason that piezoelectric coefficient (e_{31}) of $CoFe_2O_4$ is equal to zero. Also, as the value of gradient index rises, the reduction in natural frequency with respect to electric voltage becomes more significant. But, enlargement of natural frequency versus magnetic potential becomes less sensible as the gradient index increases. Therefore, properly selection of material graduation is a key issue in the successful design of MEE-FG structures.

Influence of slenderness ratio (L/h) on non-dimensional frequency of curved MEE-FG nanobeams with simply-supported edges for different values of electric voltage and magnetic potential is respectively depicted in Figs. 9 and 10 at μ = 1 nm^2, p = 1 and $\alpha = \pi/4$, $\pi/3$. It is evident that effect of electric and magnetic fields become significant at larger values of slenderness ratio. In fact, thicker MEE-FG nanobeams are less influenced by the magneto-electrical field compared to thinner MEE-FG nanobeams. It is found that negative/positive electric voltages increase /decrease the vibration frequencies of curved MEE-FG nanobeam. This is due to the compressive and tensile forces produced in the MEE-FG nanobeams via the applied positive and negative voltages, respectively. So, zero external electric voltage V = 0 makes no compressive or tensile force and will not affect the dimensionless frequency with changing of slenderness ratio. Moreover, negative/positive magnetic potentials reduce /increase the vibration frequencies of curved MEE-FG nanobeam with the changing of slenderness ratio. All these behaviors for curved MEE-FG nanobeams are dependent on the value of opening angle. So, a rise in opening angle leads to reduction in natural

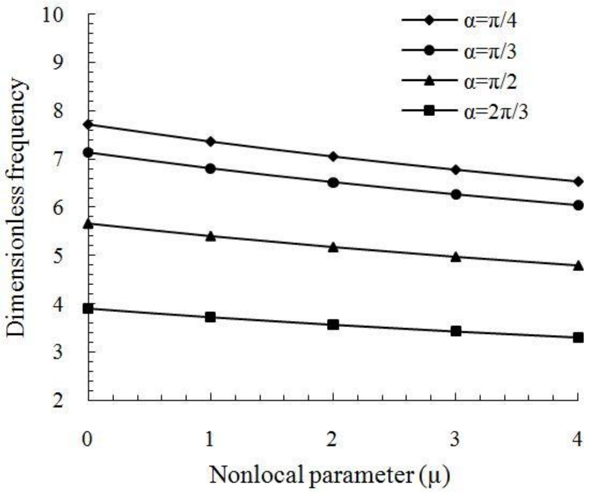

Fig. 7 Variation of dimensionless frequency of curved MEE-FG nanobeam versus electric voltage for various values of gradient index (μ = 1 nm^2, $\alpha = \pi/4$, L/h = 20)

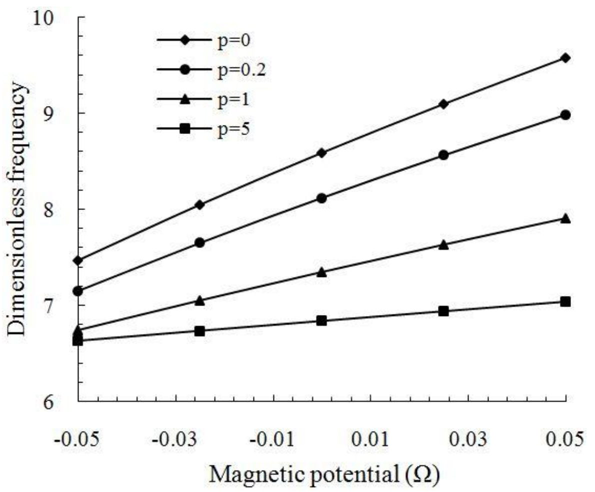

Fig. 8 Variation of dimensionless frequency of curved MEE-FG nanobeam versus magnetic potential for various values of gradient index (μ = 1 nm^2, $\alpha = \pi/4$, L/h = 20)

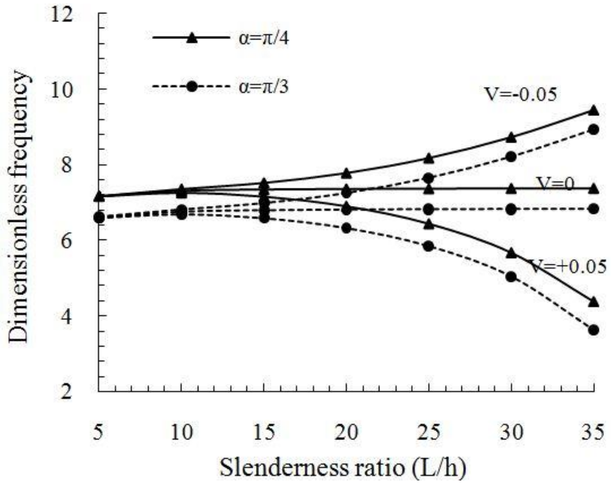

Fig. 9 Variation of dimensionless frequency of curved MEE-FG nanobeam versus slenderness ratio for various values of electric voltage (μ = 1 nm^2, p = 1)

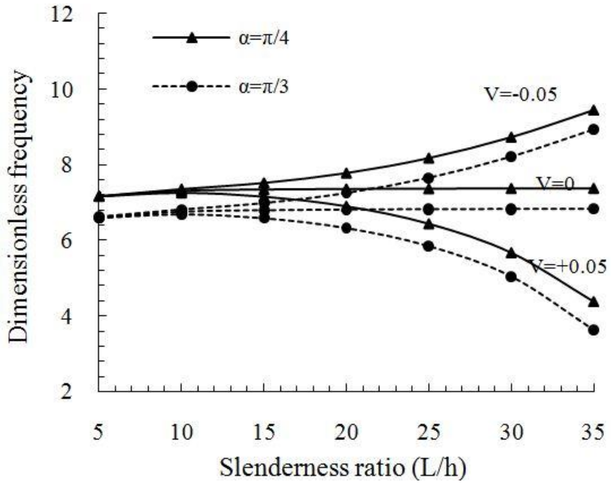

Fig. 10 Variation of dimensionless frequency of curved MEE-FG nanobeam versus slenderness ratio for various values of magnetic potential (μ = 1 nm^2, p = 1)

frequencies for every value of electric voltage, magnetic potential and slenderness ratio.

5. Conclusions

This work makes the first attempt to present a nonlocal magneto-electro-elastic curved beam model to study natural frequencies of curved MEE-FG nanobeams. The material properties of curved MEE-FG nanobeam are graded in radial direction according to the power-law model. Navier solution is applied to solve the governing equations derived from Hamilton's principle. It is found that magnetic potential, electric voltage, opening angle, nonlocal parameter, gradient index and slenderness ratio dramatically vary the natural frequencies of curved MEE-FG nanobeam. It is clear that when the radius of curved FG nanobeam extends to infinity the natural frequencies approaches to those of straight nanobeam. Also, increasing opening angle leads to lower dimensionless frequencies. The inclusion of the nonlocal parameter decreases the vibration frequency of curved MEE-FG nanobeam. Also, effect of magneto-electric field becomes significant at larger values of slenderness ratio. Negative/positive electric voltages increase/decrease the vibration frequencies of curved MEE-FG nanobeam by increasing slenderness ratio. But, negative/positive electric voltages reduce /increase the vibration frequencies with changing of slenderness ratio. Also, effect of gradient index on vibration frequencies depends on the sign and value of electric voltage and magnetic potential.

References

Assadi, A. and Farshi, B. (2011), "Size dependent vibration of curved nanobeams and rings including surface energies", *Physica E*: *Low-dimens*. *Syst*. *Nanostruct*., **43**(4), 975-978.

Aydogdu, M. (2009), "A general nonlocal beam theory: its application to nanobeam bending, buckling and vibration", *Physica E*: *Low-dimens*. *Syst*. *Nanostruct*., **41**(9), 1651-1655.

Barati, M.R., Zenkour, A.M. and Shahverdi, H. (2016), "Thermo-mechanical buckling analysis of embedded nanosize FG plates in thermal environments via an inverse cotangential theory", *Compos*. *Struct*., **141**, 203-212.

Beni, Y.T. (2016), "Size-dependent electromechanical bending, buckling, and free vibration analysis of functionally graded piezoelectric nanobeams", *J*. *Intell*. *Mater*. *Syst*. *Struct*., 1045389X15624798.

Ebrahimi, F. and Barati, M.R. (2016), "Hygrothermal buckling analysis of magnetically actuated embedded higher order functionally graded nanoscale beams considering the neutral surface position", *J*. *Thermal Stress*., **39**(10), 1210-1229.

Ebrahimi, F. and Barati, M.R. (2017a), "Buckling analysis of smart size-dependent higher order magneto-electro-thermo-elastic functionally graded nanosize beams", *J*. *Mech*., **33**(1), 23-33

Ebrahimi, F. and Barati, M.R. (2017b), "Through-the-length temperature distribution effects on thermal vibration analysis of nonlocal strain-gradient axially graded nanobeams subjected to

Ebrahimi, F. and Barati, M.R. (2017c), "Buckling analysis of piezoelectrically actuated smart nanoscale plates subjected to magnetic field", *J. Intel. Mater. Syst. Struct.*, **28**(11), 1472-1490.

nonuniform magnetic field", *J*. *Thermal Stress*., **40**(5), 548-563.

Ebrahimi, F. and Barati, M.R. (2018a), "Damping vibration behavior of visco-elastically coupled double-layered graphene sheets based on nonlocal strain gradient theory", *Microsyst*. *Technol*., **24**(3), 1643-1658.

Ebrahimi, F. and Barati, M.R. (2018b), "Vibration analysis of graphene sheets resting on the orthotropic elastic medium subjected to hygro-thermal and in-plane magnetic fields based on the nonlocal strain gradient theory", *Proceedings of the Institution of Mechanical Engineers*, *Part C*: *Journal of Mechanical Engineering Science*, **232**(13), pp. 2469-2481.

Ebrahimi, F. and Dabbagh, A. (2017a), "Nonlocal strain gradient based wave dispersion behavior of smart rotating magneto-electro-elastic nanoplates", *Mater*. *Res*. *Express*, **4**(2), 025003.

Ebrahimi, F. and Dabbagh, A. (2017b), "On flexural wave propagation responses of smart fg magneto-electro-elastic nanoplates via nonlocal strain gradient theory", *Compos*. *Struct*., **162**, 281-293.

Ebrahimi, F. and Dabbagh, A. (2017c), "Wave propagation analysis of embedded nanoplates based on a nonlocal strain gradient-based surface piezoelectricity theory", *Eur*. *Phys*. *J*. *Plus*, **132**(11), 449.

Ebrahimi, F. and Dabbagh, A. (2017d), "Wave propagation analysis of smart rotating porous heterogeneous piezo-electric nanobeams", *Eur*. *Phys*. *J*. *Plus*, **132**(4), 153.

Ebrahimi, F. and Dabbagh, A. (2018a), "Effect of humid-thermal environment on wave dispersion characteristics of single-layered graphene sheets", *Appl*. *Phys*. *A*, **124**(4), 301.

Ebrahimi, F. and Dabbagh, A. (2018b), "On modeling wave dispersion characteristics of protein lipid nanotubules", *J*. *Biomech*., **77**, 1-7.

Ebrahimi, F. and Dabbagh, A. (2018c), "On wave dispersion characteristics of double-layered graphene sheets in thermal environments", *J*. *Electromag*. *Waves Appl*., **32**(15), 1869-1888.

Ebrahimi, F. and Dabbagh, A. (2018d), "Thermo-magnetic field effects on the wave propagation behavior of smart magnetostrictive sandwich nanoplates", *Eur*. *Phys*. *J*. *Plus*, **133**(3), 97.

Ebrahimi, F. and Dabbagh, A. (2018e), "Wave dispersion characteristics of orthotropic double-nanoplate-system subjected to a longitudinal magnetic field", *Microsyst*. *Technol*., **24**(7), 2929-2939.

Ebrahimi, F. and Dabbagh, A. (2018f), "Wave dispersion characteristics of rotating heterogeneous magneto-electro-elastic nanobeams based on nonlocal strain gradient elasticity theory", *J*. *Electromag*. *Waves Appl*., **32**(2), 138-169.

Ebrahimi, F. and Dabbagh, A. (2018g), "Wave propagation analysis of magnetostrictive sandwich composite nanoplates via nonlocal strain gradient theory", *Proceedings of the Institution of Mechanical Engineers*, *Part C*: *Journal of Mechanical Engineering Science*, **232**(22), 4180-4192.

Ebrahimi, F. and Haghi, P. (2018), "Wave dispersion analysis of rotating heterogeneous nanobeams in thermal environment", *Adv*. *Nano Res*., *Int*. *J*., **6**(1), 21-37.

Ebrahimi, F. and Hosseini, S. (2016), "Thermal effects on nonlinear vibration behavior of viscoelastic nanosize plates", *J*. *Thermal Stress*., **39**(5), 606-625.

Ebrahimi, F. and Salari, E. (2015a), "A semi-analytical method for vibrational and buckling analysis of functionally graded nanobeams considering the physical neutral axis position", *CMES: Comput. Model. Eng. Sci.*, **105**(2), 151-181.

Ebrahimi, F. and Salari, E. (2015b), "Size-dependent thermo-electrical buckling analysis of functionally graded piezoelectric nanobeams", *Smart Mater. Struct.*, **24**(12), 125007.

Ebrahimi, F., Salari, E. and Hosseini, S.A.H. (2015), "Thermomechanical vibration behavior of fg nanobeams subjected to linear and non-linear temperature distributions", *J. Thermal Stress.*, **38**(12), 1360-1386.

Ebrahimi, F., Barati, M.R. and Dabbagh, A. (2016a), "A nonlocal strain gradient theory for wave propagation analysis in temperature-dependent inhomogeneous nanoplates", *Int. J. Eng. Sci.*, **107**, 169-182.

Ebrahimi, F., Barati, M.R. and Dabbagh, A. (2016b), "Wave dispersion characteristics of axially loaded magneto-electro-elastic nanobeams", *Appl. Phys. A*, **122**(11), 949.

Ebrahimi, F., Dabbagh, A. and Barati, M.R. (2016c), "Wave propagation analysis of a size-dependent magneto-electro-elastic heterogeneous nanoplate", *Eur. Phys. J. Plus*, **131**(12), 433.

Ebrahimi, F., Barati, M.R. and Haghi, P. (2017), "Thermal effects on wave propagation characteristics of rotating strain gradient temperature-dependent functionally graded nanoscale beams", *J. Thermal Stress.*, **40**(5), 535-547.

Ebrahimi, F., Barati, M.R. and Dabbagh, A. (2018a), "Wave propagation in embedded inhomogeneous nanoscale plates incorporating thermal effects", *Waves Random Complex Media*, **28**(2), 215-235.

Ebrahimi, F., Haghi, P. and Dabbagh, A. (2018b), "Analytical wave dispersion modeling in advanced piezoelectric double-layered nanobeam systems", *Struct. Eng. Mech., Int. J.*, **67**(2), 175-183.

Eringen, A.C. (1972), "Nonlocal polar elastic continua", *Int. J. Eng. Sci.*, **10**(1), 1-16.

Eringen, A.C. (1983), "On differential equations of nonlocal elasticity and solutions of screw dislocation and surface waves", *J. Appl. Phys.*, **54**(9), 4703-4710.

Hosseini, S.A.H. and Rahmani, O. (2016), "Free vibration of shallow and deep curved FG nanobeam via nonlocal Timoshenko curved beam model", *Appl. Phys. A*, **122**(3), 1-11.

Hosseini-Hashemi, S., Nahas, I., Fakher, M. and Nazemnezhad, R. (2014), "Surface effects on free vibration of piezoelectric functionally graded nanobeams using nonlocal elasticity", *Acta Mechanica*, **225**(6), 1555-1564.

Kananipour, H., Ahmadi, M. and Chavoshi, H. (2014), "Application of nonlocal elasticity and DQM to dynamic analysis of curved nanobeams", *Latin Am. J. Solids Struct.*, **11**(5), 848-853.

Li, L. and Hu, Y. (2017), "Torsional vibration of bi-directional functionally graded nanotubes based on nonlocal elasticity theory", *Compos. Struct.*, **172**, 242-250.

Li, L., Hu, Y. and Ling, L. (2015), "Flexural wave propagation in small-scaled functionally graded beams via a nonlocal strain gradient theory", *Compos. Struct.*, **133**, 1079-1092.

Li, L., Li, X. and Hu, Y. (2016), "Free vibration analysis of nonlocal strain gradient beams made of functionally graded material", *Int. J. Eng. Sci.*, **102**, 77-92.

Niknam, H. and Aghdam, M.M. (2015), "A semi analytical approach for large amplitude free vibration and buckling of nonlocal FG beams resting on elastic foundation", *Compos. Struct.*, **119**, 452-462.

Ochs, S., Li, S., Adams, C. and Melz, T. (2017), "Efficient Experimental Validation of Stochastic Sensitivity Analyses of Smart Systems", In: *Smart Structures and Materials*, Springer International Publishing, pp. 97-113.

Rahmani, O. and Jandaghian, A.A. (2015), "Buckling analysis of functionally graded nanobeams based on a nonlocal third-order shear deformation theory", *Appl. Phys. A*, **119**(3), 1019-1032.

Şimşek, M. and Yurtcu, H.H. (2013), "Analytical solutions for bending and buckling of functionally graded nanobeams based on the nonlocal Timoshenko beam theory", *Compos. Struct.*, **97**, 378-386.

Setoodeh, A., Derahaki, M. and Bavi, N. (2015), "DQ thermal buckling analysis of embedded curved carbon nanotubes based on nonlocal elasticity theory", *Latin Am. J. Solids Struct.*, **12**(10), 1901-1917.

Thai, H.T. (2012), "A nonlocal beam theory for bending, buckling, and vibration of nanobeams", *Int. J. Eng. Sci.*, **52**, 56-64.

Tufekci, E., Aya, S.A. and Oldac, O. (2016), "In-Plane Static Analysis of Nonlocal Curved Beams with Varying Curvature and Cross-Section", *Int. J. Appl. Mech.*, **8**(1), 1650010.

Vinyas, M. (2019a), "A higher order free vibration analysis of carbon nanotube-reinforced magneto-electro-elastic plates using finite element methods", *Compos. Part B*, **158**, 286-301.

Vinyas, M. (2019b), "Vibration control of skew magneto-electro-elastic plates using active constrained layer damping", *Compos. Struct.*, **208**, 600-617.

Vinyas, M. and Kattimani, S.C. (2017a), "Static studies of stepped functionally graded magneto-electro-elastic beam subjected to different thermal loads", *Composite Structures*, **163**, 216-237.

Vinyas, M. and Kattimani, S.C. (2017b), "A Finite element based assessment of static behavior of multiphase magneto-electro-elastic beams under different thermal loading", *Structural Engineering and Mechanics*, **62**, 519-535.

Vinyas, M. and Kattimani, S.C. (2017c), "Static analysis of stepped functionally graded magneto-electro-elastic plates in thermal environment: A finite element study", *Composite Structures*, **178**, 63-86.

Vinyas, M. and Kattimani, S.C. (2018a), "Finite element evaluation of free vibration characteristics of magneto-electro-elastic rectangular plates in hygrothermal environment using higher-order shear deformation theory", *Composite Structures*, **202**, 1339-1352.

Vinyas, M. and Kattimani, S.C. (2018b), "Investigation of the effect of $BaTiO_3/CoFe_2O_4$ particle arrangement on the static response of magneto-electro-thermo-elastic plates", *Composite Structures*, **185**(1), 51-64.

Vinyas, M., Kattimani, S.C., Loja, M.A.R. and Vishwas, M. (2018), "Effect of BaTiO3/CoFe2O4 micro-topological textures on the coupled static behaviour of magneto-electro-thermo-elastic beams in different thermal environment", *Mater. Res. Express*, **5**, 125702.

Vinyas, M., Nischith, G., Loja, M.A.R., Ebrahimi, F. and Duc, N.D. (2019), "Numerical analysis of the vibration response of skew magneto-electro-elastic plates based on the higher-order shear deformation theory", *Compos. Struct.*, **214**, 132-142.

Yan, Z. and Jiang, L. (2011), "Electromechanical response of a curved piezoelectric nanobeam with the consideration of surface effects", *Journal of Physics D: Applied Physics*, **44**(36), 365301.

Zhu, X. and Li, L. (2017a), "Twisting statics of functionally graded nanotubes using Eringen's nonlocal integral model", *Compos. Struct.*, **178**, 87-96.

Zhu, X. and Li, L. (2017b), "Longitudinal and torsional vibrations of size-dependent rods via nonlocal integral elasticity", *Int. J. Mech. Sci.*, **133**, 639-650.

CC